DOI: 10.1002/ejic.200800512

Sulfate-Bridged Dimeric Copper(II) Complexes with Three-Dimensional Network: Synthesis, Structure and DFT Studies

Chandrama Basu,[a] Saptashati Biswas,[a] Asoke P. Chattopadhyay,[b] Helen Stoeckli-Evans,[c] and Soma Mukherjee*[a]

Keywords: Dimeric copper(II) / Electrochemistry / Density functional calculations

The 1:1 reaction of the diacetyl monoxime-2-pyridyl hydrazone HL^1 (**1**) and the pyridine-2-carboxaldehyde-2-imidazoline hydrazone hydrobromide HL^2 (**2**) with copper(II) sulfate pentahydrate in methanol affords a series of new sulfate-bridged dimeric copper(II) complexes, $[Cu^{II}_2(HL^1)_2(\mu\text{-}SO_4)_2]\cdot 4H_2O$ (**1a**) and $[Cu^{II}_2(HL^2)_2(\mu\text{-}SO_4)Br_2]\cdot 2H_2O$ (**2a**), respectively. The room temperature magnetic moments of the complexes **1a** and **2a** are 1.82 μ_β and 1.84 μ_β, respectively. The bands appearing in the UV region (200–340 nm) are characteristic of the ligands HL^1 (**1**) and HL^2 (**2**). In complexes **1a** and **2a**, these ligand centred bands are accompanied by multiple bands extending into the visible region (370–480 nm). The association constant (K_{ass}, UV/Vis) was found to be $(1.120 \pm 0.002) \times 10^5$ for **1a** and $(1.196 \pm 0.002) \times 10^4$ for **2a** at 298 K determined using UV/Vis spectroscopy. On excitation at 285 nm, ligand **1** emits strongly in the 364 nm region due to an intraligand $^1(\pi\text{–}\pi^*)$ transition. Upon complexation with copper(II), the emission peak is slightly blue shifted (354 nm, F/F_o 0.89) with a little quenching in the emission intensity as expected for divalent copper. Complexes **1a** and **2a** exhibit two consecutive oxidation couples for two copper(II) centres in deionised distilled water under a nitrogen atmosphere. DFT and TDDFT calculations were performed and the results are highly consistent with the spectroscopic behaviour of the complexes. The molecular structures of dinuclear **1a** (Cu···Cu 4.555 Å) and **2a** (Cu···Cu 6.106 Å) have been determined by single-crystal X-ray diffraction studies.

Introduction

Transition-metal-based frameworks are particularly interesting because of various useful biological and technological applications that may arise from their special electronic, magnetic, ion exchange, adsorption, photochemical and catalytic properties.[1–19] The properties can be varied by changing the ligand type, the presence of substituents and by using different metal ions. Introduction of spacers and/or bridging ligands[20–30] between two redox active metal termini not only permits the electron flow essential for construction of nanoscale devices [31–33] but also significantly influences the overall topology of the framework. Among inorganic anions, sulfates are particularly interesting since they are capable of binding metal centres in a bidentate, tridentate or bridging mode.[34–38] Sulfate-bridged dinuclear copper complexes with substituted imidazoles and *N*-heteroaromatic receptors are of great importance because of their wide applicability in synthetic, biological and supramolecular chemistry.[39–46] The above objective has been realised with the synthesis, characterisation and employment of new homodinuclear copper(II) complexes with active redox centres. Interestingly, the modulation of the ligand frame has a remarkable influence on the photophysical as well as the binding patterns of the complexes. Emphasis will be given to understand the binding phenomenon by means of the binding constant and thermodynamic calculations for the complexation equilibrium. DFT and TDDFT calculations were performed to establish the nature of the orbitals involved in transition processes and to correlate the structural parameters with the spectroscopic properties of the complexes.[47–53]

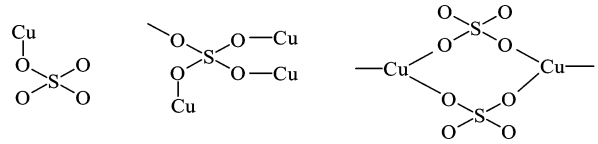

[a] Department of Environmental Science, University of Kalyani, Kalyani, Nadia 741235, West Bengal, India
Fax: +91-33-2582-8282
E-mail: sommukh445@yahoo.co.in
[b] Department of Chemistry, University of Kalyani, Kalyani, Nadia 741235, West Bengal, India
[c] Institute of Microtechnology, University of Neuchâtel, Rue Emile Argand 11, 2009 Neuchâtel, Switzerland
Supporting information for this article is available on the WWW under http://www.eurjic.org or from the author.

Results and Discussion

The ligands HL^1 (**1**) and HL^2 (**2**) react with copper(II) sulfate pentahydrate in methanol at room temperature in a 1:1 molar ratio to afford green dinuclear copper(II) com-

plexes of the type $[Cu_2(HL^1)_2(\mu\text{-}SO_4)_2]\cdot 4H_2O$ (**1a**) and $[Cu_2(HL^2)_2(\mu\text{-}SO_4)Br_2]\cdot 2H_2O$ (**2a**), respectively, in excellent yields.

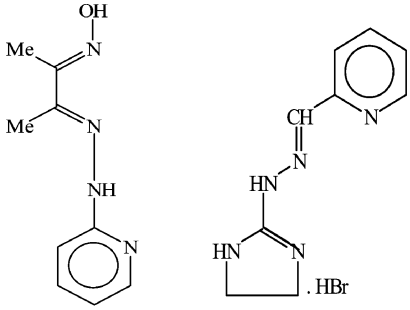

HL^1, **1** HL^2, **2**

The elemental analysis data are consistent with the proposed empirical formulae. All the complexes are soluble in methanol but sparingly soluble in water. The binding modes of **1**, and **2**, are shown below. The room temperature magnetic moments of complexes **1a** and **2a** are 1.82 μ_β and 1.84 μ_β, respectively. These values are consistent with an $S = ½$ spin state as expected for d^9 ($t_2^6e^3$) systems.

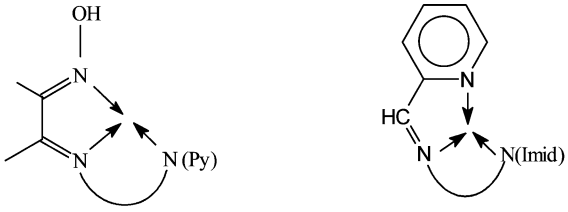

HL^1, **1** HL^2, **2**

Crystal Structures of 1a and 2a

The molecular structures of the dinuclear complexes $[Cu_2(HL^1)_2(\mu\text{-}SO_4)_2]\cdot 4H_2O$ (**1a**) and $[Cu_2(HL^2)_2(\mu\text{-}SO_4)Br_2]\cdot 2H_2O$ (**2a**) together with their schematic representations are shown in Figures 1 and 3, respectively. Crystal packing diagrams illustrating the different hydrogen bonding in the two structures are shown in Figures 2 and 4 and selected bond lengths and angles are listed in Tables 1 and 2. Details of the hydrogen bonding are given in Table 3.

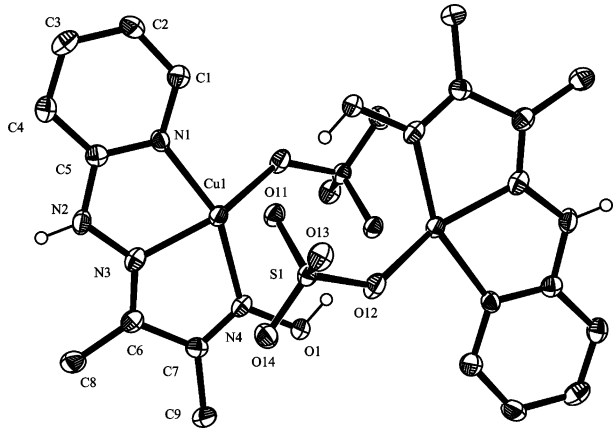

Figure 1. Molecular structure of complex $[Cu_2(HL^1)_2(\mu\text{-}SO_4)_2]\cdot 4H_2O$ (**1a**) with thermal ellipsoids drawn at the 50% probability level. Water molecules have been omitted for clarity.

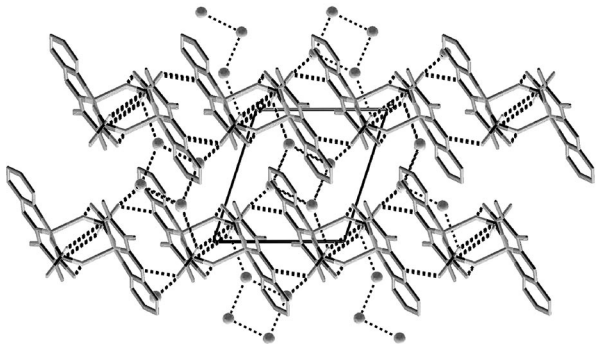

Figure 2. Crystal packing diagram of $[Cu_2(HL^1)_2(\mu\text{-}SO_4)_2]\cdot 4H_2O$ (**1a**) viewed along the *c* axis, showing the inter- and intramolecular hydrogen bonding (dotted lines). The hydrogen atoms are not shown for clarity.

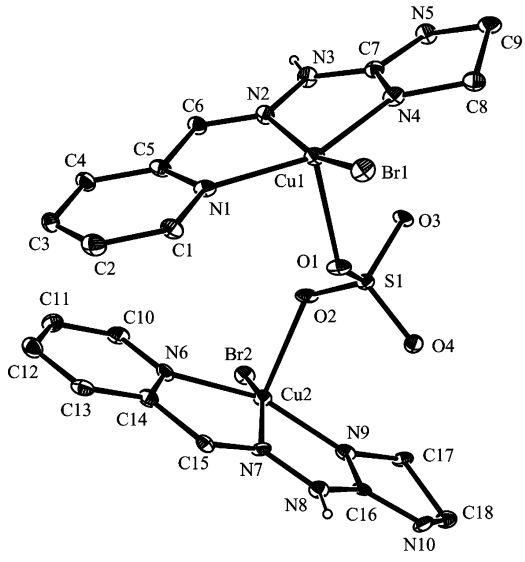

Figure 3. Molecular structure of the complex $[Cu_2(HL^2)_2(\mu\text{-}SO_4)\text{-}Br_2]\cdot 2H_2O$ (**2a**) with thermal ellipsoids drawn at the 50% probability level. The water molecules are not shown for clarity.

Table 1. Selected bond lengths [Å] and angles [°] for $[Cu_2(HL^1)_2(\mu\text{-}SO_4)_2]\cdot 4H_2O$ (**1a**).

Complex **1a**			
Cu(1)–N(1)	1.995(3)	Cu(1)–N(3)	1.943(3)
Cu(1)–N(4)	2.032(3)	Cu(1)–O(11)	2.196(3)
Cu(1)–O(12a)	1.955(3)		
N(1)–Cu(1)–N(4)	157.24(13)	N(3)–Cu(1)–N(1)	79.55(13)
N(3)–Cu(1)–N(4)	78.11(12)	N(1)–Cu(1)–O(11)	96.28(12)
N(3)–Cu(1)–O(11)	113.60(11)	N(3)–Cu(1)–O(12a)	153.26(13)
N(4)–Cu(1)–O(11)	96.54(10)	O(12a)–Cu(1)–N(1)	92.29(12)
O(12a)–Cu(1)–N(4)	105.85(11)	O(12a)–Cu(1)–O(11)	92.47(10)

Symmetry operation a: *–x*, *–y*, *–z* + 1

Table 2. Selected bond lengths [Å] and angles [°] for $[Cu_2(HL^2)_2(\mu\text{-}SO_4)Br_2]\cdot 2H_2O$ (**2a**).

Complex, **2a**			
Cu(1)–Br(1)	2.386(2)	Cu(1)–N(4)	1.956(11)
Cu(1)–N(1)	2.058(11)	Cu(1)–O(1)	2.274(10)
Cu(1)–N(2)	2.000(11)	Cu(2)–Br(2)	2.379(2)
Cu(2)–N(6)	2.066(12)	Cu(2)–N(7)	2.000(11)
Cu(2)–N(9)	1.950(12)	Cu(2)–O(2)	2.283(9)
N(1)–Cu(1)–Br(1)	98.8(3)	N(2)–Cu(1)–Br(1)	160.5(3)
N(4)–Cu(1)–Br(1)	99.7(4)	O(1)–Cu(1)–Br(1)	103.0(3)
N(2)–Cu(1)–N(1)	78.2(4)	N(4)–Cu(1)–N(1)	155.5(5)
N(4)–Cu(1)–N(2)	79.0(5)	N(1)–Cu(1)–O(1)	90.6(4)
N(2)–Cu(1)–O(1)	96.4(4)	N(4)–Cu(1)–O(1)	100.7(4)
N(6)–Cu(2)–Br(2)	99.0(3)	N(7)–Cu(2)–Br(2)	160.1(3)
N(9)–Cu(2)–Br(2)	99.6(3)	O(2)–Cu(2)–Br(2)	103.1(2)
N(7)–Cu(2)–N(6)	77.8(4)	N(9)–Cu(2)–N(6)	155.6(4)
N(9)–Cu(2)–N(7)	79.4(5)	N(6)–Cu(2)–O(2)	90.7(4)
N(7)–Cu(2)–O(2)	96.6(4)	N(9)–Cu(2)–O(2)	100.3(4)

Cu(1)–O(11) 2.196(3) Å, Cu(1)–O(12a) 1.995(3) Å [symmetry operation, a: $-x, -y, -z + 1$]. The Cu1···Cu1a distance, in the case of the bisulfate-bridged material, is ca. 4.555 Å. Atoms N1, N3, N4 and O12a define the basal plane, with atom O11 occupying the axial position. The angles at the metal centre between the *cis*-positioned donor pairs span the range 78.11(12)°–113.60(11)° and those between the *trans* positioned pairs are 153.26(13)° and 157.24(13)°. The copper atom is displaced by 0.302(1) Å from the best mean-plane (RMS = 0.137) through the basal plane atoms towards atom O11 of the sulfate. The hydroxy substituent oxygen O1 is hydrogen-bonded to O11 of the sulfate group and they are related by the centre of symmetry. The coordinated water molecule is also involved in an intramolecular hydrogen bond with a sulfate O-atom, O14. In the crystal structure of **1a**, water molecules O1w and O2w are hydrogen-bonded to each other and to the sulfate atoms O1 and O13. A layer-like structure is formed in the *ac* plane and these layers are connected by the water molecules to form a 3D hydrogen-bonded structure (Figure 2 and Table 3).

Table 3. Hydrogen bonding distances [Å] and angles [°] in compounds **1a** and **2a**.

Complex **1a**				
D–H···A	D–H	H···A	D···A	D–H···A
O(1)–H(1).O(11a)	0.84	1.83	2.663(4)	170
O(1 W) – H(1WA).O(14b)	0.83(4)	2.10(4)	2.915(4)	169(3)
N(2)–H(2).O(13c)	0.88	2.00	2.759(5)	144
O(1 W)–H(1WB).O(1b)	0.84(6)	2.56(6)	3.189(4)	133(5)
O(2 W)–H(2WA).O(1Wd)	0.84(6)	2.14(6)	2.822(5)	138(5)
O(2 W)–H(2WA).O(1Wd)	0.82(4)	2.05(5)	2.795(5)	153(5)
O(2 W)–H(2WB).O(13)	0.84(5)	2.08(5)	2.901(4)	168(5)
Symmetry operations a: $-x, -y, 1 - z$; b: $1 + x, 1 + y, z$; c: $1 + x, y, z$; d: $1 - x, 1 - y, - z$				
Complex **2a**				
D–H···A	D–H	H···A	D···A	D–H···A
O(1 W) – H1WA.Br1a	0.88(7)	2.64(6)	3.464(16)	155(10)
9(OW)–H(1WB).O(3b)	0.88(16)	1.86(16)	2.719(19)	163.00
N(3)–H(3N).O(3c)	0.88	1.84	2.695(15)	162
O(2 W)–H(2WB).Br(2d)	0.89(14)	2.78(12)	3.472(15)	136(16)
O(2 W)–H(2WA).O(4b)	0.9(2)	1.98(19)	2.735(19)	141(16)
N(8)–H(8N).O(4e)	0.88	1.85	2.703(15)	163
C(3)–H(3).Br(2d)	0.95	2.92	3.656(15)	135
C(6)–H(6).O(1Wf)	0.95	2.44	3.34(2)	156
C(9)–H(9a).O(1Wg)	0.99	2.57	2.97(2)	104
C(15)–H(15).O(2Wh)	0.95	2.47	3.37(2)	157
C(18) – H(18a).O(2Wi)	0.99	2.56	2.97(2)	104
Symmetry operations a: $x, -1 + y, z$; b: $1 + x, -1 + y, z$; c: $-x, 2 - y, 1 - z$; d: $1 + x, y, z$; e: $-x, 2 - y, -z$; f: $1 - x, 1 - y, 1 - z$; g: $1 - x, 2 - y, 1 - z$; h: $1 - x, 1 - y, -z$; i: $-x, 1 - y, -z$				

$[Cu_2(HL^1)_2(\mu\text{-}SO_4)_2]\cdot 4H_2O$ (1a)

The molecular structure of **1a** clearly shows that it is a centrosymmetric disulfate-bridged dimeric Cu^{II}–Cu^{II} complex with a $[Cu_2(\mu\text{-}SO_4)_2]$ core unit (Figure 1). Each copper atom lies in a square pyramidal N_3O_2 coordination environment with a 3D euclidian geometry and is connected to the other by means of two sulfate groups bridging in an end-to-end fashion. The ligand binds to the metal in a tridentate manner utilising the pyridyl, imine and oxime N-atoms as potential donor sites with bond distances of Cu(1)–N(1) 1.955(3) Å, Cu(1)–N(3) 1.943(3) Å, Cu(1)–N(4) 2.032(3) Å, respectively. The penta-coordination of the copper atoms is completed by two oxygen atoms from the two sulfate ions,

$[Cu_2(HL^2)_2(\mu\text{-}SO_4)Br_2]\cdot 2H_2O$ (2a)

The molecular structure of **2a** (Figure 3) clearly shows a 3D euclidian geometry. Each metal atom is connected to the other by means of a sulfate group bridging in an end-to-end fashion. Each copper atom has a pentacoordinate N_3OBr environment (three nitrogen atoms from the ligand, one bromide ion and one oxygen atom from the sulfate ion)

thus forming a [$Cu_2(\mu\text{-}SO_4)$] core unit. The Cu1···Cu2 distance is 6.106 Å. For the coordination sphere of Cu1, atoms N1, N2, N4 and Br1 define the basal plane while sulfate atom O1 occupies the axial position [Cu(1)–N(1) 2.058(11) Å, Cu(1)–N(2) 2.000(11) Å, Cu(1)–N(4) 1.956(11) Å, Cu(1)–Br(1) 2.386(2) Å, and Cu(1)–O(1) 2.274(10) Å]. The angles at Cu1 between the *cis*-positioned donor pairs span the range 78.2(4)°–103.0(3)° and those between the *trans*-positioned pairs are 155.5(5)° and 160.5(3)°. For the coordination sphere of Cu2, atoms N6, N7, N9 and Br2 define the basal plane while sulfate atom O2 occupies the axial position [Cu(2)–N(6) 2.066(12) Å, Cu(2)–N(7) 2.000(11) Å, Cu(2)–N(9) 1.950(12) Å, Cu(2)–Br(2) 2.379(2) Å, Cu(2)–O(2) 2.283(9) Å]. The angles at Cu2 between the *cis* positioned donor pairs span the range 77.8(4)° – 103.1(2)° and those between the *trans* positioned pairs are 155.6(4)° and 160.1(3)°. Hence the geometry of both five coordinated copper atoms is slightly distorted 3D euclidian. Atom Cu1 is displaced by 0.297(1) Å from the best mean-plane (RMS = 0.071) through the basal plane atoms in the direction of the axial atom O1. Atom Cu2 is displaced by 0.297(1) Å from the best mean-plane (RMS = 0.077) through the basal plane atoms in the direction of the axial atom O2. In the crystal structure of **2a**, symmetry-related molecules are connected by O–H···Br, O–H···O and N–H···O hydrogen bonds, which leads to the formation of a 3D structure (Figure 4 and Table 3).

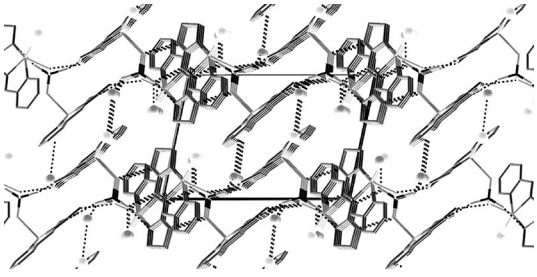

Figure 4. Crystal packing diagram of [$Cu_2(HL^2)_2(\mu\text{-}SO_4)\ Br_2$]·$2H_2O$ (**2a**), viewed along the *b* axis and showing the intermolecular hydrogen bonding (dotted lines). The hydrogen atoms are not shown for clarity.

Spectroscopic Studies

All the spectroscopic measurements were carried out in degassed methanol at room temperature. The bands appearing in the UV region 200–340 nm are characteristic of the ligands, HL^1 (**1**) and HL^2 (**2**). In the complexes [$Cu_2(HL^1)_2(\mu\text{-}SO_4)_2$]·$4H_2O$ (**1a**) and [$Cu_2(HL^2)_2(\mu\text{-}SO_4)Br_2$]·$2H_2O$ (**2a**) these ligand centred bands are accompanied by multiple bands extending into the visible region (370–480 nm). On excitation at 285 nm, ligand **1** strongly emits at 364 nm due to an intraligand $^1(\pi\text{–}\pi^*)$ transition. Upon complexation with copper(II) the emission peak is slightly blue shifted (354 nm) with a little quenching in the emission intensity as expected for divalent copper.[54] The ratio of fluorescence intensity of complex **1a** in the presence of metal (F) and in the absence of metal (F_o) is 0.89. On modulation of the ligand frame as in **2**, the emission property is completely lost as revealed from the DFT calculation (vide supra) and therefore its dinuclear sulfate-bridged copper(II) complex **2a** becomes nonfluorescent.

Thermodynamics of Binding

The association constant (K_{ass}) of complexes **1a** and **2a** can be estimated spectrophotometrically according to Equation (1)[18,55] where X represents the absorption intensity, X_{lim} represents the absorption intensity at full complexation, C_0 is the initial concentration of the ligand, C_H and C_G are the corresponding concentrations of the ligand and metal ion during titration. The K_{ass} (UV/Vis) was found to be $(1.120 \pm 0.002) \times 10^5$ for the complex **1a** and $(1.196 \pm 0.002) \times 10^4$ for **2a** at 298 K. A representative diagram is shown in Figure 5.

$$X = X_o + (X_{lim} - X_o)/2\,C_0\,\{C_H + C_G + 1/K_{ass} - [(C_H + C_G + 1/K_{ass})^2 - 4\,C_H C_G]^{1/2}\} \quad (1)$$

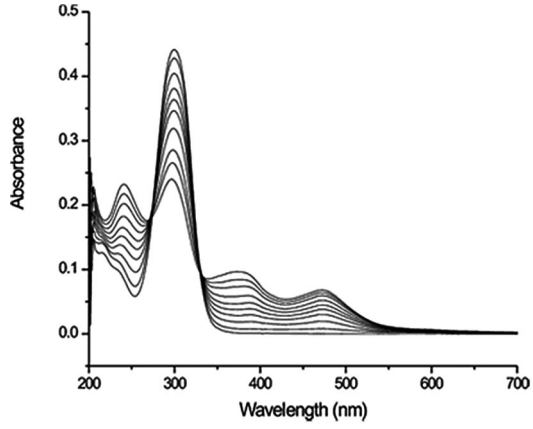

Figure 5. Absorbance spectra of HL^1 (**1**) (1.0×10^{-5} M) upon addition of copper(II) (1.0×10^{-6} M – 1.0×10^{-5} M) in degassed methanol (pH = 7.0) at 298 K.

The high Dq value of oximato N-coordination is probably the main reason for the enhanced stability of complex **1a** compared to **2a**.[56–58] The temperature dependence of the binding constant was studied between 293 K and 308 K and the values of the thermodynamic parameters for the binding were obtained by variable-temperature UV/Vis titration in degassed methanol at 298 nm. The standard Gibb's energy change, ΔG^0, the standard enthalpy change, ΔH^0 and the standard entropy change, ΔS^0 which are listed in Table 4 were calculated using van 't Hoff's Equation. It can be seen that the binding process is favoured by the negative ΔH^0 and positive ΔS^0.

Table 4. Thermodynamic parameters for the complexes **1a** and **2a**.

Complexes	K_{ass}	ΔG^0 [cal mˆ ı]	ΔH^0 [cal mˆ ı]	ΔS^0[cal mˆ ı deg^{-1}]
$[Cu_2(HL^1)_2(\mu\text{-}SO_4)_2]\cdot 4H_2O$ (**1a**)	$(1.120 \pm 0.002) \times 10^5$	–6929.35±1.27	–324 ± 4.01	22.17 ± 0.045
$[Cu_2(HL^2)_2(\mu SO_4)Br_2]\cdot 2H_2O$ (**2a**)	$(1.196 \pm 0.002) \times 10^4$	–5596.33±5.06	–45.77 ± 4.27	18.63 ± 0.012

Metal Redox

The redox properties of the complexes **1a** and **2a** have been studied in doubly distilled deionised water by cyclic voltammetry using a platinum working electrode. The dimeric copper(II) complexes **1a** and **2a** exhibit two consecutive oxidative responses Ox_I and Ox_{II} on the positive side of the Ag/AgCl electrode under a nitrogen atmosphere. The dimeric complex, **1a** displays a quasi reversible (ΔE_p = 160 mV) one-electron cyclic response near 0.35 V which was assigned to the Cu(II/II)/Cu(II/III) oxidation. In case of complex **2a**, the first oxidative response can be observed at 0.45 V (ΔE_p = 160 mV). The high ligand field-strength of the oximato *N*-coordination (vide infra)[56–58] is probably the main reason for the lowering of the redox potential in **1a** (0.35 V) compared with **2a** (0.45 V) vs. the Ag/AgCl electrode. In both the cases the second oxidative response for Cu(II/III)/Cu(III/III) is irreversible. In all cases the potential values are lower than the reported $E_{1/2}$ Cu(II/III) values.[59] We were unable to isolate the oxidised species in pure form due to their instability at a higher potential.

Electronic Structure Calculations and Correlation with Spectroscopic Transitions

In the present work, DFT and time-dependent DFT (TDDFT) calculations were carried out on the X-ray crystallographic data of the complexes $[Cu_2(HL^1)_2(\mu\text{-}SO_4)_2]\cdot 4H_2O$ (**1a**) and $[Cu_2(HL^2)_2(\mu\text{-}SO_4)Br_2]\cdot 2H_2O$ (**2a**) and on the gas phase structures of corresponding ligands, HL^1 and HL^2. The highest occupied (HOMO) and the lowest unoccupied (LUMO) molecular orbitals are abbreviated as H and L, respectively, and other orbitals are referred accordingly. Figure 6 gives the energy level diagram of sets of MOs of all the ligands and complexes relevant for our study and Figure 7 shows some MO pictures of complexes **1a** and **2a**.

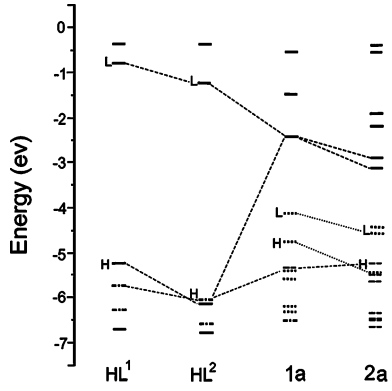

Figure 6. Frontier MO levels of ligands **HL¹**, **HL²** and complexes **1a** and **2a** [dot-dash (-·-): ligand σ levels; dots (···): copper d levels; dashes (---): ligand SO_4^{-2} and/or Br levels; solid lines (—): ligand π levels].

For the fluorescent ligand **1** most of the MOs are π orbitals, except H-1 and H-2 (–5.74, –6.31 eV). The latter are lone pairs, centred on N1, N2 and N4 of the ligand. The H at –5.27 eV is a π chain from N3 to well inside the pyridine while the L, at –0.8 eV, extends from C6 via N3 to the pyridine (as shown in Figure 1).

For the nonfluorescent ligand **2** the four lowest virtual orbitals (L to L + 3) are all π* orbitals. L and L + 1 (–1.26, –0.38 eV) extend from pyrrole to pyridine. The H at

$[Cu_2(HL^1)_2(\mu\text{-}SO_4)_2]\cdot 4H_2O$ (**1a**)

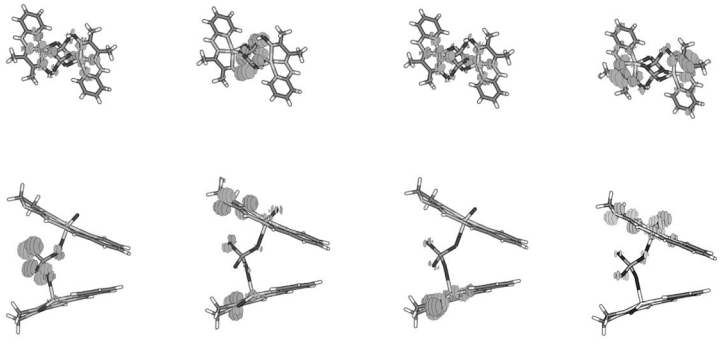

$Cu_2(HL^2)_2(\mu\text{-}SO_4)Br_2]\cdot 2H_2O$ (**2a**)

Figure 7. Some MO pictures (HOMO, HOMO – 1, LUMO, LUMO + 1) of $[Cu_2(HL^1)_2(\mu\text{-}SO_4)_2]\cdot 4H_2O$ (**1a**) and $[Cu_2(HL^2)_2(\mu\text{-}SO_4)Br_2]\cdot 2H_2O$ (**2a**).

–6.07 eV is a σ type orbital which constitutes the backbone of the ligand and H-2 is similar to H. H-1 and H-3 (–6.16, –6.77 eV) are π orbitals.

Compared with the ligands, the complexes **1a** and **2a** exhibit a denser set of MOs. In **1a**, H and L (–4.79, –4.16 eV) consist of mixed Cu(3d) and O(2p) orbitals. The four MOs below H (–5.42, –5.42, –5.46, –5.61 eV) mainly originate from the two sulfate bridges with H-3 and H-4 having some Cu(3d) mixed in it. Orbitals further down originate from the ligands. Below these, H-5 (–6.21 eV) and H-6 (–6.35 eV) are quite close in energy and both constitute Cu(3d) + SO_4^{2-} type ML orbitals. H-9 at –6.56 eV is similar in nature. In between, the nearly degenerate H-7 (–6.50 eV) and H-8 (–6.53 eV) form the imine N3, N2, C5 and some of the pyridine and Cu(3d) (Figure 1). L + 1 and L + 2 (–2.45, –2.43 eV) are ligand π* orbitals excluding the pyridine and the adjacent imine N2. The higher energy orbitals all originate from the pyridine of the ligand.

For the nonfluorescent complex **2a**, H (–5.25 eV) is a sulfate orbital but L and L + 1 (–4.60, –4.46 eV) are both mixed Cu(3d) and ligand π* orbitals. L + 2 and L + 3 (–3.15, –2.92 eV) are ligand π* orbitals. Orbitals still higher in energy mostly originate from the pyridine moiety. The orbitals H-1 to H-4 (–5.42, –5.42, –5.45, –5.68 eV) all originate from the sulfate group with H-1 and H-2 having some contributions from Cu(3d) and the pyridine as well. The next set of quasi-degenerate occupied orbitals, H-5 to H-9 (–6.37 to –6.77 eV) are essentially bromine (4p) orbitals.

Thus the fluorescent ligand HL^1 (**1**) and complex **1a** can be distinguished by the similar nature (π or Cu + ligand π) of the HOMO and LUMO. For the nonfluorescent ligand HL^2 (**2**) and complex **2a** these orbitals are not similar in nature. In the case of **2** the HOMO is a σ-type and the LUMO is a π*-type orbital. For **2a**, the HOMO is a sulfate orbital while the LUMO has both Cu(3d) and neighbouring ligand components.

A comparison of the TDDFT results as shown in Table 5 and the experimental data is quite revealing. We only report high oscillator strength (*f*, in brackets) transitions found in our calculations in the UV/Vis region. For the fluorescent ligand HL^1 the calculated transitions are π–π*-type at 223.77 nm, 284.12 nm and 306.14 nm, made up of components such as H-3→L, H→L + 2 etc. The values are in close agreement with observed λ_{max} values at 298 nm and 215 nm. For the nonfluorescent ligand HL^2 (**2**) the calculated transitions were at 316.2 nm and 337.53 nm while observed values were at 204 nm, 298 nm and 332 nm. The calculated values correspond to π–π* transitions, the main components being H-1→L, H-1→L + 1 etc. In case of the fluorescent complex $[Cu_2(HL^1)_2(\mu\text{-}SO_4)_2]\cdot 4H_2O$ (**1a**) the observed transitions at 204, 241, 294, 370 and 471 nm may be compared with the TDDFT values of 230.36, 278.51, 319.42 and 450.83 nm. The first two transitions are of the ML to ML type whereas the next two are primarily of the $L(SO_4^{-2})$→ML-type. The transitions for the nonfluorescent complex $[Cu_2(HL^2)_2(\mu\text{-}SO_4)Br_2]\cdot 2H_2O$ (**2a**) were found to be at 199.65, 238.95, 285.28 and 446.30 nm. These values compare well with experimental λ_{max} values at 205, 237, 295 and 409 nm. All these transitions for compound **2a** are of the L→ML-type where the ligand orbitals are mainly SO_4^{-2}, except for the calculated transition at 238.95 nm where bromine and pyridine also contribute.

An attempt was also made to reproduce the fluorescence spectra of the ligand, HL^1 (**1**) using TDDFT calculations. The calculation involved transitions $S_0 \rightarrow S_1$ and $S_1 \rightarrow S_0$ from optimised S_0 and S_1 states, respectively. The partially converged results for absorption and emission were $\lambda_{ex}(S_0 \rightarrow S_1)$ at 328.85 nm and $\lambda_{em}(S_1 \rightarrow S_0)$ at 381.58 nm, respectively. The calculated λ_{em} value compares favourably with observed λ_{em} value (364 nm). The nonfluorescent nature of the ligand HL^2 is due to the intrusion of a non π (σ) type orbital as the HOMO between the π and π* orbitals

Table 5. List of selected transition wavelengths (oscillator strength) and the major contributions of **1**, **2**, **1a** and **2a**, calculated in the gas phase by the TDDFT method (percentages are given in brackets).

λ_{max} [nm]	Oscillator strength ($f \times 10^3$)	Major contribution
223.77	88.70	HL^1 (**1**)
		H-3→L + 1(28),H→L + 2(25.7), H-3→L(24.8), H-5→L + 1(7)
284.12	341.94	H→L + 1(71.6), H→L(14.1)
306.14	176.38	H→L(68.3), H→L + 1(19.8)
		HL^2 (**2**)
316.20	14.78	H-4→L(66.1), H-5→L(16.1), H-2→L + 1(4.6)
337.53	0.39	H-1→L + 1(46.9), H→L(44.9), H-2→L + 1(5.5)
		$[Cu_2(HL^1)_2(\mu\text{-}SO_4)_2]\cdot 4H_2O$ (**1a**)
230.36	10.03	H→L(48.2), H-3→L(36.1) ML→ML
278.51	0.69	H→L(23), H-3→L(27.6), H-9→L(24.8), H-4→L(15.3) ML→ML
319.42	1.47	H-3→L(40.5), H-4→L(37.9), H→L(10.4) L→ML
450.83	0.58	H-3→L(31.80), H-4→L(26.2), H-9→L(20.7), H→L(9.6) L→ML
		$[Cu_2(HL^2)_2(\mu\text{-}SO_4)Br_2]\cdot 2H_2O$ (**2a**)
199.65	7.32	H→L(46.3), H-2→L(43.8), H-3→L(7.6) $L(SO_4^{2-})$→ML
238.95	8.51	H-6→L(34.6), H-3→L(26.6), H-5→L(16), H-2→L(4.5)
		H-1→L + 1(4.4) L→ML
285.28	0.12	H→L(46.8), H-2→L(31.6), H-3→L(6.6) L→ML
446.30	3.74	H-1→L (double excitation) (81.6) L→ML

(Figure 6). The fluorescent complex was too large to be handled in the same manner. The interesting information revealed in the present study necessitates further investigation in these and related complexes. Such studies are in progress.

Conclusions

A series of dinuclear copper(II) (S = ½) complexes **1a** and **2a** based on ligand **1** and **2** have been successfully designed and synthesised. Modulation of the ligand frames significantly influences the photophysical and chemical properties of the complexes. The association constants (K_{ass}) and thermodynamic calculations clearly revealed that in all cases the binding process is favoured by a negative ΔH^0 and a positive ΔS^0. The complexes exhibit metal centred oxidative response for Cu^{II}/Cu^{III} in aqueous media under a nitrogen atmosphere. The increased K_{ass} value and low redox potential in **1a** may be due to the high Dq value of the oximato-N. The DFT and TDDFT calculations are quite useful in establishing the electronic structures and spectroscopic transitions of the ligands and complexes. The X-ray structures show that the ligands bind the metal in a tridentate manner resulting in the 3D euclidian geometry in all cases. The Cu···Cu distance in **1a** is ca. 4.555 Å and that in complex **2a** is 6.106 Å. Complexes **1a** and **2a** also display strong intra- and intermolecular H-bonding leading to the formation of 3D networks.

Experimental Section

Materials: All starting materials and solvents were purchased from Sigma Aldrich Chemical Company and used without further purification unless otherwise stated.

Physical Measurements: A Perkin–Elmer 2400 C Elemental Analyser was used to collect microanalytical data (C, H, N). A Sartorius CP64 balance was used for weighing. IR data were collected using an FTIR Perkin–Elmer L 120-000 A instrument. The UV/Vis spectra of the ligand and its complexes were recorded on a Shimadzu UV-1601 spectrophotometer and corrected for the background resulting from the solvent absorption. Fluorescence spectra were recorded with a Perkin–Elmer LS 50B Luminescence spectrometer. All spectroscopic measurements were carried out in degassed HPLC grade methanol at room temperature. For binding constant measurements, solutions were prepared at fixed concentrations of HL^1 (**1**) and HL^2 (**2**) (1.0×10^{-5} M) and at a concentration of metal ions ranging from $(1.0–10.0) \times 10^{-6}$ M at room temperature. Electrochemical measurements were performed under a nitrogen atmosphere on a Versastat II PAR Electrochemistry system using a platinum electrode. NH_4PF_6 was used as a supporting electrolyte and the potentials are referenced to the Ag/AgCl electrode. Room temperature magnetic susceptibilities were measured with a model 155 PAR vibrating sample magnetometer fitted with a Walker Scientific L75FBAL magnet.

Syntheses of Ligands and Complexes

The ligands and complexes were synthesised and then characterised by various analytical techniques including C,H,N analysis, FTIR, absorption and emission spectroscopy, magnetic and redox measurements, and single-crystal X-ray diffraction studies. DFT calculations were also performed.

HL^1 (1): Ligand **1** was synthesised by the same general procedure as before.[60] $C_9H_{12}N_4O$ (192): calcd. C 56.25, H 6.25, N 29.16; found C 56.26, H 6.23, N 29.15. FTIR: $\tilde{\nu}$ = 3335, 3153, 3017, 2801, 1965, 1912, 1609, 1574, 1527, 1513, 1445, 1360, 1309, 1276, 1168, 1144, 1093, 1045, 1015, 998, 980, 928, 860, 767, 734, 695, 634, 592, 574, 551, 505, 459, 412 cm^{-1}. UV/Vis (CH_3OH): λ_{max} (ε, $M^{-1}cm^{-1}$): 298 (42800), 215 (12600) nm.

HL^2 (2): The new ligand was prepared by 1:1 condensation of pyridine-2-carbaldehyde (0.021 g, 0.2 mmol) and 2-hydrazino-2-imidazoline hydrobromide (0.036 g, 0.2 mmol) in methanol. On recrystallisation from methanol, pale yellow crystals separated out which were dried with fused $CaCl_2$. Yield 0.044 g, 82%. $C_9H_{12}BrN_5$ (270): calcd. C 40.00, H 4.07, N 25.92; found C 40.01, H 4.08, N 25.90. FTIR: $\tilde{\nu}$ = 3551, 3473, 3414, 3233, 3097, 3029, 2970, 2890, 1657, 1616, 1585, 1566, 1516, 1489, 1470, 1433, 1380, 1365, 1292, 1233, 1191, 1145, 1130, 1070, 1000, 930, 882, 781, 745, 660, 621, 517, 479 cm^{-1}. UV/Vis (CH_3OH): λ_{max} (ε, $M^{-1}cm^{-1}$): 332 (24300), 298 (43500), 204 (19800) nm.

$[Cu_2(HL^1)_2(\mu\text{-}SO_4)_2]\cdot 4H_2O$ (1a): To a methanolic solution of copper(II) sulfate pentahydrate (0.04 g, 0.2 mmol) was added a solution of HL^1 (**1**) (0.038 g, 0.2 mmol) in methanol (5 mL) and the resultant green solution was stirred for 0.5 h. The solvent was evaporated using a rotary evaporator and on recrystallisation from methanol, dark green crystals of $[Cu_2(HL^1)_2(SO_4)_2]\cdot 4H_2O$ (**1a**) were obtained; yield 0.065 g, 84%. $C_{18}H_{24}Cu_2N_8O_{10}S_2\cdot 4H_2O$ (775.72): calcd. C 27.84, H 4.12, N 14.43; found C 27.86, H 4.13, N 14.44. FTIR: $\tilde{\nu}$ = 3423, 3259, 3149, 3064, 3055, 2952, 2877, 2761, 1618, 1571, 1506, 1477, 1423, 1380, 1321, 1288, 1257, 1226, 1141, 1118, 1035, 1014, 902, 829, 771, 744, 619, 572, 509, 459, 416 cm^{-1}. UV/Vis (CH_3OH): λ_{max} (ε, $M^{-1}cm^{-1}$): 471 (8110), 370 (11340), 294 (17370), 241 (25900), 204 (23610) nm.

$[Cu_2(HL^2)_2(\mu\text{-}SO_4)Br_2]\cdot 2H_2O$ (2a): Copper(II) sulfate pentahydrate (0.04 g, 0.2 mmol) in methanol (5 mL) was added to a methanolic solution (5 mL) of HL^2, **2** (0.05 g, 0.2 mmol) with constant stirring. A green coloured solution was obtained which, on slow evaporation, yielded a shining greenish-brown crystalline solid of $[Cu_2(HL^2)_2(\mu\text{-}SO_4)Br_2]\cdot 2H_2O$ (**2a**); yield 0.067 g, 85%. $C_{18}H_{20}Br_2Cu_2N_{10}O_6S\cdot 2H_2O$ (795.43): calcd. C 27.15, H 3.01, N 17.60; found C 27.16, H 3.02, N 17.58. FTIR: $\tilde{\nu}$ = 3240, 3080, 2956, 2891, 1649, 1618, 1575, 1558, 1512, 1467, 1352, 1336, 1280, 1217, 1122, 1078, 1043, 1020, 923, 779, 675, 649, 621, 603, 580, 557, 518, 497, 472, 449, 422 cm^{-1}. UV/Vis (CH_3OH), λ_{max} (ε, $M^{-1}cm^{-1}$): 409 (9300), 295 (22400), 237 (17700), 205 (34700) nm.

X-ray Structure Determination of 1a and 2a: Diffraction data for single crystals of **1a** and **2a** (**1a**, dark green, $0.12 \times 0.23 \times 0.38$ mm; **2a**, greenish brown $0.37 \times 0.14 \times 0.12$ mm) were grown by slow evaporation of methanol at 298 K. The intensity data were collected at 173 K on a Stoe Image Plate Diffraction System[61] equipped with a two-circle goniometer using Mo-K_α-monochromated radiation (λ = 0.71073 Å). The structures were solved by Direct Methods using the program SHELXS-97.[62] The refinement and all further calculations were carried out using SHELXL-97.[62] The H atoms were either located from Fourier difference maps and refined isotropically or included in calculated positions and treated as riding atoms using SHELXL default parameters. The water H-atoms were refined in most cases with distance restraints. The non-hydrogen atoms were refined anisotropically using weighted full-matrix least-squares on $|F^2|$. Further crystallographic data and details of the refinement are given in Table 6.

Table 6. Crystallographic data and structure refinement for compounds **1a** and **2a**.

	1a	**2a**
Formula	$C_{18}H_{24}Cu_2N_8O_{10}S_2{\cdot}4H_2O$	$C_{18}H_{20}Br_2Cu_2N_{10}O_6S{\cdot}2H_2O$
Formula Mass	775.72	795.43
T [K]	173(2)	173(2)
Wavelength [Å]	0.71073	0.71073
Crystal system	triclinic	triclinic
Space group	$P\bar{1}$	$P\bar{1}$
a [Å]	8.5160(11)	9.837(2)
b [Å]	8.6027(11)	9.838(2)
c [Å]	10.7487(14)	14.333(3)
α [°]	97.193(16)	99.423(16)
β [°]	109.374(15)	99.440(16)
γ [°]	104.371(15)	101.276(16)
V [Å^3]	700.82(19)	1314.1(5)
Z	1	2
$D_{calcd.}$ [g cm^{-3}]	1.838	2.010
μ [mm^{-1}]	1.750	4.795
F(000)	398	788
Crystal dimensions [mm]	$0.12 \times 0.23 \times 0.38$	$0.37 \times 0.14 \times 0.12$
θ Range [°]	2.7–26.0	1.47–25.20
Limiting indices	–10/10; –10/10; –13/13	–11/11; –11/11; –17/17
Reflections collected / unique	5524 / 2546	11186 / 4665
Refinement method	full-matrix least squares on F^2	
Data / restraints / parameters	2546 /6 / 218	4665 / 4 / 364
GOF on F^2	0.991	1.235
R_1,[a] wR_2[b] [$I > 2\sigma(I)$]	0.0445, 0.1189	0.0627, 0.2085
R_1,[a] wR_2[b] (all data)	0.0532, 0.1355	0.1099, 0.2189
Largest diff. peak and hole [e Å^{-3}]	–0.85, 0.96	–0.761, 0.901

[a] $R_1 = [\Sigma||F_o| - |F_c||]/\Sigma |F_o|$(based on F). [b] $wR_2 = [[\Sigma w (|F_o^2 - F_c^2|)^2]/[\Sigma w(F_o^2)^2]]^{1/2}$ (based on F^2).

CCDC-686158 (for **1a**) and -686159 (for **2a**) contain the supplementary crystallographic data for this paper. These data can be obtained free of charge from The Cambridge Crystallographic Data Centre via www.ccdc.cam.ac.uk/data_request/cif.

DFT Calculations

For comparison, DFT calculations were carried out on the single-crystal X-ray structures of $[Cu_2(HL^1)_2(\mu\text{-}SO_4)_2]{\cdot}4H_2O$ (**1a**) and $[Cu_2(HL^2)_2(\mu\text{-}SO_4)Br_2]{\cdot}2H_2O]$ (**2a**) and the gas-phase structures of the corresponding ligands HL^1 (**1**) and HL^2 (**2**). The GAMESS–US [Version 2006, Sep 7 (R4)][63] and NWChem. (Version 4.5)[64] packages were used for the calculations. The valence-only SBKJC basis set[65] and B3LYP functional[66] were used. Electronic transitions were checked using the TDDFT method in both packages. The MO pictures and molecular structures were obtained with MOLDEN[67] software.

Supporting Information (see also the footnote on the first page of this article): Luminescence spectra of ligand **HL^1** (**1**) and complex $[Cu_2(HL^1)_2(\mu\text{-}SO_4)_2]{\cdot}4H_2O$ (**1a**), Tables S1 and S2 containing raw data regarding the determination of K_{ass}.

Acknowledgments

Financial support received from the Department of Science and Technology, New Delhi and the Council of Scientific and Industrial Research, New Delhi are gratefully acknowledged. S. M. and S. B. are grateful to the Indo-Swiss Bilateral Reserach Inititive (2007) of the Swiss National Science Foundation for financing their stay at the University of Neuchâtel. We are grateful to the University of Kalyani for providing infrastructural facilities.

[1] P. C. Ford, E. Cariati, J. Bourassa, *Chem. Rev.* **1999**, *99*, 3625–3648.
[2] K. Selmeczi, M. Reglier, M. Giorgi, G. Speier, *Coord. Chem. Rev.* **2003**, *245*, 191–201.
[3] D. B. Rorabacher, *Chem. Rev.* **2004**, *104*, 651–697.
[4] C. Liu, M. Wang, T. Zhang, H. Sun, *Coord. Chem. Rev.* **2004**, *248*, 147–168.
[5] A. L. Gavrilova, B. Bosnich, *Chem. Rev.* **2004**, *104*, 349–384.
[6] L. M. Mirica, X. Ottenwaelder, T. D. P. Stack, *Chem. Rev.* **2004**, *104*, 1013–1045.
[7] E. A. Lewis, W. B. Tolman, *Chem. Rev.* **2004**, *104*, 1047–1076.
[8] H. Groove, T. L. Kelley, L. K. Thompson, L. Zhao, Z. Xu, T. S. M. Abedin, D. O. Miller, A. E. Goeta, C. Wilson, J. A. K. Howard, *Inorg. Chem.* **2004**, *43*, 4278–4288.
[9] S.-B. Zhao, R.-Y. Wang, S. Wang, *Inorg. Chem.* **2006**, *45*, 5830–5840.
[10] F. J. J. R. da Silva, R. J. P. Williams, *The Biological Chemistry of Elements: The Inorganic Chemistry of Life*, Oxford University Press, Oxford, **2001**.
[11] S. Das, P. Banerjee, S.-M. Peng, G.-H. Lee, J. Kim, S. Goswami, *Inorg. Chem.* **2006**, *45*, 562–570.
[12] R. A. Mathews, C. S. Rossiter, J. R. Marrow, J. P. Richard, *Dalton Trans.* **2007**, 3804–3811.
[13] R. Murugavel, R. Pothiraja, N. Gogoi, R. Clerac, L. Lecren, R. J. Butcher, M. Nethaji, *Dalton Trans.* **2007**, 2405–2410.
[14] N. A. Rey, A. Neves, A. J. Bortoluzzi, C. T. Pich, H. Terenzi, *Inorg. Chem.* **2007**, *46*, 348–350.
[15] G. W. Gokel, *Comprehensive Supramolecular Chemistry*, vol. 1, *Molecular Recognition: Receptors for Cationic Guests*, Pergamon, Elmsford, NY, **1996**.
[16] B. Valeur, *Molecular Fluorescence Principles and Applications*, Wiley-VCH, Verlag GmbH, Weinheim, Germany, **2001**.
[17] H. J. Schneider, A. K. Yatsimirsky, *Principles and Methods in Supramolecular Chemistry*, John Wiley & Sons, New York, **2000**.
[18] C. Basu, S. Chowdhury, R. Banerjee, H. Stoeckli-Evans, S. Mukherjee, *Polyhedron* **2007**, *26*, 3617–3624.

[19] D. Maiti, J. S. Woertink, A. A. N. Sarjeant, E. I. Solomon, K. D. Karlin, *Inorg. Chem.* **2008**, in press and references cited therein.
[20] M. Du, Y.-M. Guo, X.-H. Bu, J. Ribas, M. Monfort, *New J. Chem.* **2002**, *26*, 645–650.
[21] D. Li, S. Li, D. Yang, J. Yu, J. Huang, Y. Li, W. Tang, *Inorg. Chem.* **2003**, *42*, 6071–6080.
[22] E. A. Lewis, W. B. Tolman, *Chem. Rev.* **2004**, *104*, 1047 and references cited therein.
[23] T. Osako, Y. Ueno, Y. Tachi, S. Itoh, *Inorg. Chem.* **2004**, *43*, 6516–6518.
[24] M. Fondo, A. M. Garcia-Deibe, N. Ocampo, M. R. Bermejo, A. L. Llamas-Saiz, *Dalton Trans.* **2006**, 4260–4270.
[25] S. Shit, P. Talukdar, J. Chakraborty, G. Pilet, M. S. El Fallah, J. Ribas, S. Mitra, *Polyhedron* **2007**, *26*, 1357–1363.
[26] C. Adhikary, D. Mal, R. Sen, A. Bhattacharjee, P. Gutlich, S. Chaudhuri, S. Koner, *Polyhedron* **2007**, *26*, 1658–1662.
[27] S. Jie, M. Agostinho, A. Kermagoret, C. S. J. Cazin, P. Braustein, *Dalton Trans.* **2007**, 4472–4482.
[28] S. Sen, S. Mitra, D. L. Hughes, G. Rosair, C. Desplanches, *Polyhedron* **2007**, *26*, 1740–1744.
[29] A. Bienko, J. K. Al, J. Mrozinski, R. Boca, I. Brudgam, H. Harti, *Dalton Trans.* **2007**, 2681–2688.
[30] S.-L. Ma, X.-X. Sun, S. Gao, C.-M. Qi, H.-B. Huang, W.-X. Zhu, *Eur. J. Inorg. Chem.* **2007**, 846–851.
[31] F. Paul, C. Lapinte, *Coord. Chem. Rev.* **1998**, *178–180*, 431–509.
[32] R. Ziessel, M. Hissler, A. El-Ghayoury, A. Harriman, *Coord. Chem. Rev.* **1998**, *178–180*, 1251–1298.
[33] F. Barigelletti, L. Flamigni, *Chem. Soc. Rev.* **2000**, *29*, 1–12.
[34] Y. Okubo, A. Okamura, K. Imanishi, J. Tachibana, K. Umakoshi, Y. Sasaki, T. Okamura, *Bull. Chem. Soc. Jpn.* **1999**, *72*, 2241–2247.
[35] B. Greener, S. P. Foxon, P. H. Walton, *New J. Chem.* **2000**, *24*, 269–273.
[36] N. Lah, I. K. Cigic, I. Leban, *Inorg. Chem. Commun.* **2003**, *6*, 1441–1444.
[37] S. G. Telfer, T. Sato, T. Harada, R. Kuroda, J. Lefebvre, D. L. Leznoff, *Inorg. Chem.* **2004**, *43*, 6168–6176.
[38] A. H. I. Venkato Jr., A. J. Bortuluzzi, V. Drago, M. A. Novak, A. Neves, *J. Braz. Chem. Soc.* **2006**, *17*, 1584–1593.
[39] T. D. Hamilton, G. S. Papaefstathiou, L. R. MacGillivray, *Cryst. Eng. Comm.*. **2002**, *4*, 223–226.
[40] X.-M. Ouyang, Z.-W. Li, T. Okamura, Y.-Z. Li, W.-Y. Sun, W. X. Tang, N. Ueyama, *J. Solid State Chem.* **2004**, *177*, 350–360.
[41] L. K. Thompson, Z. Xu, A. E. Goeta, J. A. K. Howard, H. J. Clase, D. O. Miller, *Inorg. Chem.* **1998**, *37*, 3217–3229.
[42] H. Araki, K. Tsuge, Y. Sasaki, S. Ishizaka, N. Kitamura, *Inorg. Chem.* **2005**, *44*, 9667–9675.
[43] S. G. Telfer, T. Sato, T. Harada, R. Kuroda, J. Lefebvre, D. B. Leznoff, *Inorg. Chem.* **2004**, *43*, 6168–6176.
[44] H. Ohtsu, I. Shinobu, S. Nagatomo, T. Kitagawa, S. Ogo, Y. Watanabe, S. Fukuzumi, *Chem. Commun.* **2000**, 1051 and references cited therein.
[45] Y.-K. He, Z.-B. Han, *Acta Crystallogr., Sect. E* **2006**, *62*, m2676-m2677.
[46] K. K. Sarker, D. Sardar, K. Suwa, J. Otsuki, C. Sinha, *Inorg. Chem.* **2007**, *46*, 8291–8301 and references cited therein.
[47] A. Ghosh, I. Halvorsen, H. J. Nilsen, E. Steene, T. Wondimagegn, R. Lie, E. Caemelbecke, N. Guo, Z. On, K. M. Kadish, *J. Phys. Chem. B* **2001**, *105*, 8120–8124.
[48] S. Triki, C. J. Gomez-Garcia, E. Ruiz, J. Sala-Pala, *Inorg. Chem.* **2005**, *44*, 5501–5508.
[49] P. L. Holland, C. J. Cramer, E. C. Wilkinson, S. Mahapatra, K. R. Rodgens, S. Itoh, M. Taki, S. Fukuzumi, L. Que Jr., W. B. Tolman, *J. Am. Chem. Soc.* **2000**, *122*, 792–802.
[50] S. Demeshko, S. Dechert, F. Meyer, *J. Am. Chem. Soc.* **2004**, *126*, 4508–4509.
[51] P. Comba, Y. D. Lampeka, A. I. Prikhod'ko, G. Rajaraman, *Inorg. Chem.* **2006**, *45*, 3632–3638.
[52] S. Kababya, J. Nelson, C. Calle, F. Neese, D. Goldfarb, *J. Am. Chem. Soc.* **2006**, *128*, 2017–2029.
[53] E. C. Brown, A. M. Aboelella Reynolds, G. Aullon, S. Alvarez, W. B. Tolman, *Inorg. Chem.* **2004**, *43*, 3335–3337.
[54] a) F. Feng, X. Liao, Z. Chen, S. Lin, S. Meng, Z. Lu, *Anal. Chim. Acta* **2006**, *575*, 68–75; b) B. Dutta, P. Bag, K. Nag, *New J. Chem.* **2005**, *29*, 1182–1188.
[55] a) J. Valeur, J. Pouger, J. Bourson, *J. Phys. Chem.* **1992**, *96*, 6545–6549; b) L. Wang, X.-J. Zhu, W.-Y. Wong, J.-P. Guo, W.-K. Wong, Z.-Y. Li, *Dalton Trans.* **2005**, 3235–3240.
[56] a) A. Chakravorty, *Coord. Chem. Rev.* **1974**, *13*, 1–46; b) K. Pramanik, S. Karmakar, S. B. Chaudhury, A. Chakravorty, *Inorg. Chem.* **1997**, *36*, 3562–3564; c) S. Karmakar, S. B. Chaudhury, S. Ganguly, A. Chakravorty, *J. Chem. Soc., Dalton Trans.* **1997**, 585–590; d) K. Nag, A. Chakravorty, *Coord. Chem. Rev.* **1980**, *33*, 87–147.
[57] R. I. Haines, A. Mc Auley, *Coord. Chem. Rev.* **1981**, *39*, 77–119.
[58] C. Basu, S. Chowdhury, S. Mukherjee, *Indian J. Chem.* **2006**, *45A*, 1126–1131.
[59] a) M. Taki, S. Itoh, S. Fukuzumi, *J. Am. Chem. Soc.* **2002**, *124*, 998–1002; b) M. A.-Z. Eltayeb, Y. Sulfab, *Polyhedron* **2007**, *26*, 1–5.
[60] M. A. Kabil, M. A. Akl, M. E. Khalifa, *Anal. Sci.* **1999**, *15*, 433–438.
[61] Stoe, **2000**, *IPDS Software*, Stoe & Cie GmbH, Darmstadt, Germany.
[62] G. M. Sheldrick, *Acta Crystallogr., Sect. A* **2008**, *64*, 112–122.
[63] a) E. J. Bylaska, W. A. de Jong, N. Govind, K. Kowalski, T. P. Straatsma, M. Valiev, D. Wang, E. Apra, T. L. Windus, J. Hammond, P. Nichols, S. Hirata, M. T. Hackler, Y. Zhao, P.-D. Fan, R. J. Harrison, M. Dupuis, D. M. A. Smith, J. Nieplocha, V. Tipparaju, M. Krishnan, Q. Wu, T. Van Voorhis, A. A. Auer, M. Nooijen, E. Brown, G. Cisneros, G. I. Fann, H. Fruchtl, J. Garza, K. Hirao, R. Kendall, J. A. Nichols, K. Tsemekhman, K. Wolinski, J. Anchell, D. Bernholdt, P. Borowski, T. Clark, D. Clerc, H. Dachsel, M. Deegan, K. Dyall, D. Elwood, E. Glendening, M. Gutowski, A. Hess, J. Jaffe, B. Johnson, J. Ju, R. Kobayashi, R. Kutteh, Z. Lin, R. Littlefield, X. Long, B. Meng, T. Nakajima, S. Niu, L. Pollack, M. Rosing, G. Sandrone, M. Stave, H. Taylor, G. Thomas, J. van Lenthe, A. Wong, Z. Zhang, *NWChem, A Computational Chemistry Package for Parallel Computers*, version 5.1, Pacific Northwest National Laboratory, Richland, Washington 99352-0999, USA, **2007**; modified version: R. A. Kendall, E. Aprà, D. E. Bernholdt, E. J. Bylaska, M. Dupuis, G. I. Fann, R. J. Harrison, J. Ju, J. A. Nichols, J. Nieplocha, T. P. Straatsma, T. L. Windus, A. T. Wong, *Comput. Phys. Commun*. **2000**, *128*, 260–283.
[64] a) P. J. Hay, W. R. Wadt, *J. Chem. Phys.* **1985**, *82*, 270–283; b) W. R. Wadt, P. J. Hay, *J. Chem. Phys.* **1985**, *82*, 284–298; c) P. J. Hay, W. R. Wadt, *J. Chem. Phys.* **1985**, *82*, 299–310.
[65] A. D. Becke, *J. Chem. Phys.* **1993**, *98*, 5648–5652.
[66] Molden: A Pre and Post-processing Program for Molecular and Electronic Structures: G. Schaftenaar, J. H. Noordik, *J. Comput.-Aided Mol. Design* **2000**, *14*, 123–134.
[67] C. Gaiddon, P. Jeannequin, P. Biscoff, M. Pfeffer, C. Sirlin, J. P. Loeffler, *J. Pharmacol. Exp. Ther.* **2005**, *315*, 1403–1411.

Received: May 23, 2008
Published Online: September 17, 2008

